

# Vortex Control Technique for the Attenuation of Fin Buffet

David E. Bean,\* Douglas I. Greenwell,† and Norman J. Wood‡  
*University of Bath, Bath, England, United Kingdom*

The application of tangential leading edge blowing (TLEB) to reduce levels of single-fin buffeting has been studied. The tests were performed at the University of Bath 2.1 × 1.5 m wind tunnel, using two cropped 60-deg delta wings. To measure the unsteady pressures on the fin surface, a rigid fin instrumented with miniature differential pressure transducers was used. A flexible fin of similar planform and size was used to measure the buffeting response. Steady-state static pressure data and laser light sheet flow visualization were employed to aid interpretation of the vortical flow over the wings, and hence, identify the causes of the buffeting. The profiles of the unsteady pressures and the buffeting response were found to match each other very closely. It was observed that symmetric leading-edge blowing modified the leading-edge vortices by reducing the "effective angle of attack" of the vortex. Blowing at a constant rate shifted the buffet excitation and response to higher angles of attack. Flow visualization confirmed that the mechanism at peak buffeting had not changed, but had been merely shifted. It has been shown that the use of an optimum blowing profile could completely suppress the buffeting response without impairing the wing lift characteristics.

## Nomenclature

$C_\mu$	= blowing momentum coefficient, jet momentum/ $qS$
$\bar{c}$	= wing mean aerodynamic chord
$f$	= frequency
$K$	= reduced frequency, $f\bar{c}/U_\infty$
$m$	= generalized mass
$\sqrt{nG(n)}$	= buffet excitation parameter
$\bar{p}$	= rms pressure fluctuation
$q$	= freestream dynamic pressure
$S$	= wing reference area
$S_f$	= fin reference area
$U_\infty$	= tunnel freestream velocity
$z$	= fin tip acceleration, rms
$\alpha$	= angle of attack
$\zeta$	= total damping (fraction of critical)

## Introduction

HIGH angle of attack and poststall maneuvering continues to be a factor in the design of future generation combat aircraft.<sup>1,2</sup> It is anticipated that future combat aircraft will be required to maintain controlled flight in the high angle-of-attack regime for extended periods.

Severe fin buffeting has been encountered on this type of aircraft (both single- and twin-finned) during operation at high angles of attack. From wind-tunnel tests performed on such aircraft,<sup>3-8</sup> the buffeting has been attributed to vortex flow enveloping the fin(s), which excites the natural frequencies of the fin structure. This phenomenon not only decreases the fatigue life of the airframe, but may, in turn, limit the angle-of-attack envelope of the aircraft. Clearly, this is an undesirable situation which must be considered early in the design of advanced combat aircraft.

The purpose of this article is to introduce a different method of buffet suppression using the concept of tangential leading edge blowing (TLEB). Preliminary investigations have been

performed by Mabey and Pyne<sup>9</sup> to assess the merit of TLEB for buffet alleviation for a single-finned aircraft configuration. Although the wing leading edge (and therefore, the jet profile) was not ideal, the system provided some buffeting reduction. It was also noted that the system gave a slight improvement in the drag at high angles of attack. Therefore, TLEB has potential for buffeting suppression at high angles of attack while providing improvements in aircraft performance.

Recent studies at the University of Bath have confirmed the ability of TLEB to control the vortical flowfield on delta wings in the poststall region.<sup>10</sup> The present study includes measurements of buffet levels on a flexible fin and unsteady pressures on a rigid fin of similar planform for both unblown and blown 60-deg delta wings. Laser light sheet flow visualization and force/moment balance tests have been conducted to clarify the mechanisms for buffeting reductions using TLEB.

## TLEB

There have been several attempts to control the vortical flow over a delta wing by blowing.<sup>11-14</sup> The ability of many of these techniques to modify the leading-edge vortices has been proven at prestall angles of attack, but not at poststall conditions.

Previous research has demonstrated the ability of TLEB to modify vortical flowfields and to provide lateral control at both prestall and poststall angles of attack.<sup>15,16</sup> TLEB is an application of the phenomenon of Coanda jet attachment to convex surfaces.

If the leading edge of a delta wing is sharp, the leading-edge separation point is fixed, and the vortex equilibrium condition is influenced only by the vortex strength and position for a given angle of attack. However, if the leading edge is rounded, the separation point is able to move around the leading edge, providing an additional degree of freedom (DOF) on the flowfield. Therefore, there exists a unique vortex strength and location for each leading-edge separation point at a constant angle of attack. By injecting a thin tangential jet into the crossflow boundary layer near the leading edge (see Fig. 1), further control of the boundary-layer separation is provided by the momentum of the jet, so the jet enables control of the vortex equilibrium condition at a given angle of attack.

At low angles of attack, the effect of TLEB is to reduce the leading-edge vortex strength and relocate the vortex in-

Received May 15, 1992; revision received Aug. 3, 1992; accepted for publication Aug. 3, 1992. Copyright © 1992 by the American Institute of Aeronautics and Astronautics, Inc. All rights reserved.

\*Research Officer, School of Mechanical Engineering. Member AIAA.

†Research Officer, School of Mechanical Engineering.

‡Senior Lecturer, School of Mechanical Engineering. Member AIAA.

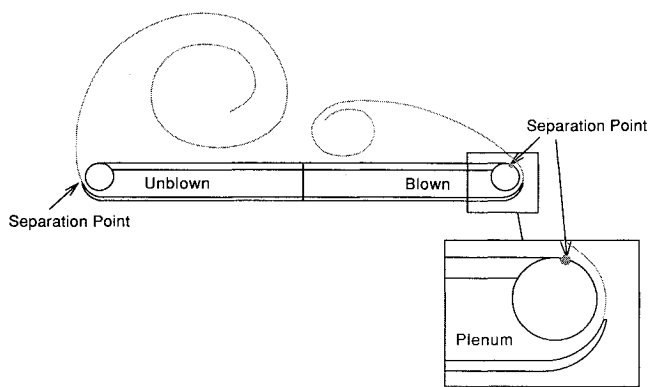


Fig. 1 Tangential leading-edge blowing. Leading-edge blowing affects the vortex equilibrium condition by control of the location of the separation point.

board with negligible reduction in wing normal force. At post-stall angles of attack, blowing moves the vortex burst points aft and augments the wing normal force. TLEB can be considered as reducing the "effective angle of attack" of the vortex, i.e., at fixed incidence, increasing blowing momentum modifies the vortical flow to represent that at a lower angle of attack.

## Experimental Apparatus

### Model Support System

A model support system has been designed to be used in the  $2.1 \times 1.5$  m tunnel at the University of Bath, specifically for research into high angle-of-attack aerodynamics (Fig. 2). The rig is a pantograph mechanism mounted on its side with pitch control provided by an electric linear actuator which provides a pitch range from 0 to 90 deg. The model is sting-mounted on an "A-frame" layout to give maximum lateral stiffness, and model forces and moments are measured by a three-component strain gauge sting balance.

Glass panels in the tunnel walls provide laser access, and all Scanivalve tubing, instrumentation wires, and blowing air supplies are passed inside the A-frames.

A more complete description of the model support system may be obtained from Ref. 17.

### Wind-Tunnel Models

Two models of similar planform and size, one with and one without TLEB, have been built and tested to determine the effects of TLEB on buffeting response. Both models are 60-deg delta wings of 0.5-m span and 0.53-m chord, with a trailing-edge extension for fin attachment (Fig. 3). The unblown wing has a rounded leading edge, 4% thickness, and is fitted with 90 upper surface pressure tapings situated at  $x/c = 0.30, 0.45, 0.59,$  and  $0.73$ .

The blown wing is 3% thick and has two separate plenum chambers providing the blowing supply for the slots which extend over the majority of the leading edges. The plenum pressures are monitored separately by miniature pressure transducers and are manually controlled. The leading-edge-slot height is adjustable from 0.0 to 1.0 mm, and may vary along the slot length. Previous experience has shown that TLEB is most efficient when a linear tapered slot is used<sup>18</sup> (tapering towards the wing apex). This slot configuration gives results that are easiest to interpret, as the vortical flow responds quasiconically. Two slot configurations were tested: 1) a linearly tapering slot, and 2) a constant width slot.

The buffeting response was measured using a flexible fin whose natural frequencies were designed using the following reduced frequencies (based on wing mean aerodynamic chord and half the maximum tunnel velocity): bending (1st mode),  $K = 0.6-0.8$ ; and torsion (1st mode),  $K = 2.0-3.0$ .

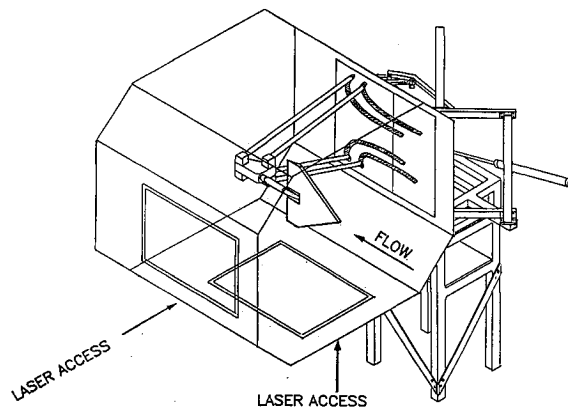


Fig. 2 High angle-of-attack model support system in the  $2.1 \times 1.5$  m low-speed wind tunnel.

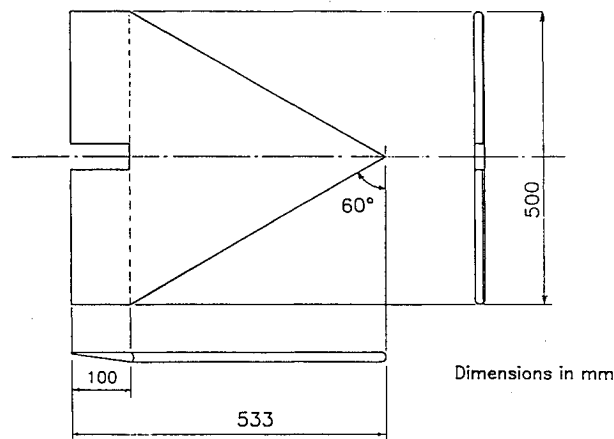


Fig. 3 Planform of wings tested.

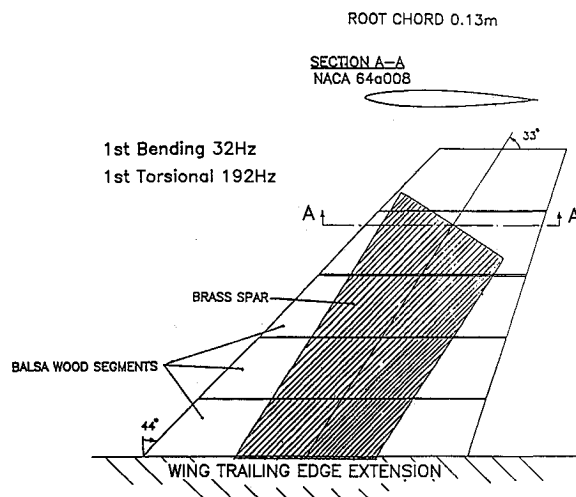


Fig. 4 Flexible fin design.

These reduced frequencies are typical of a modern combat aircraft. The frequency term in this expression is the frequency of the natural mode (and therefore, unrelated to the excitation frequency). The flexible fin is shown in Fig. 4. It consists of a thin brass spar surrounded by a balsa wood shroud to provide an aerodynamic fairing and the correct fin area. Fin vibration levels were sensed by root strain gauges instrumented in half-bridge circuits.

The fin used to detect the excitation pressures was rigid, manufactured from aluminum, and of similar planform and section to the flexible fin. A miniature differential pressure transducer was mounted on each face of the fin at 75% span and 40% chord, to monitor the pressure fluctuations in the

flow. Insufficient transducers were available for more detailed coverage of the fin surface.

Both fins were rigidly fixed to the trailing-edge extensions of the models. Typical test Reynolds numbers were  $0.8 \times 10^6$  based on wing root chord.

Laser light sheet flow visualization was used to help understand the phenomenon of buffeting. Laser access was by way of the wind-tunnel door and floor windows, with smoke injected on the lower surfaces of the wings adjacent to the leading edge. Images were obtained using both a 35-mm camera and a low-light level video camera.

#### Data Acquisition and Reduction

On-line data acquisition and reduction of the strain gauge balance data and steady-state pressures was performed using a data acquisition program "Rigtest" developed at the University of Bath. The program was written specifically to control the DT2821® data acquisition board (by Data Translation, Inc.), which was installed on a desktop computer. The steady pressures were measured by two standard J-type Scanivalves. All data was displayed graphically in coefficient form immediately after being acquired.

The unsteady data (from the strain gauges and pressure transducers) was gathered using a commercially available data acquisition package (Global Lab® by Data Translation, Inc.) which controlled a DT2821 data acquisition board. After acquisition, the data could be manipulated (using Global Lab's extensive analysis library) and saved as postprocessed results.

The fin excitation and response data were nondimensionalized in order to enable comparison between different test configurations. The response (strain gauge) data was reduced into the nondimensional buffet parameter<sup>19</sup>:

$$\sqrt{nG(n)} = \frac{2mz}{\sqrt{\pi q S_f}} \sqrt{\zeta}$$

The generalized mass was determined using modal analysis. A known impulse was applied to the fin structure using an instrumented hammer, and a light accelerometer sensed the natural modes present. The mass term for each natural mode was then derived from the spectra of both signals. The relationship between tip acceleration and root strain was determined using a modal solution for a flat plate cantilever.

Buffeting spectra were obtained from within Global Lab using a fast Fourier transformation size corresponding to 6–7 s of raw data. The total damping values (typically 2–3%) were derived using the half-power method and were found to be independent of freestream speed, indicating that the damping was predominantly structural.

The excitation pressure data was nondimensionalized into the form

$$\bar{p}/q$$

where  $\bar{p}$  is the total broadband rms pressure fluctuation. This parameter represents the oscillatory nature of the flow at the fin surface.

#### Results and Discussion

All results presented correspond to buffeting tests at zero wing sideslip and a reduced frequency of 0.6 (based on the fin first bending and wing mean aerodynamic chord), except where stated.

##### Without TLEB

The single-fin response in the fundamental bending mode (32 Hz) is shown in Fig. 5. The heavy buffet criterion as defined by Mabey<sup>15</sup> is added for comparison. For low angles of attack the response is small, the vortices lie away from the fin, and the fin excitation is a result of general flow unsteadiness. At  $\alpha = 34$  deg (a point called "buffet onset") the buf-

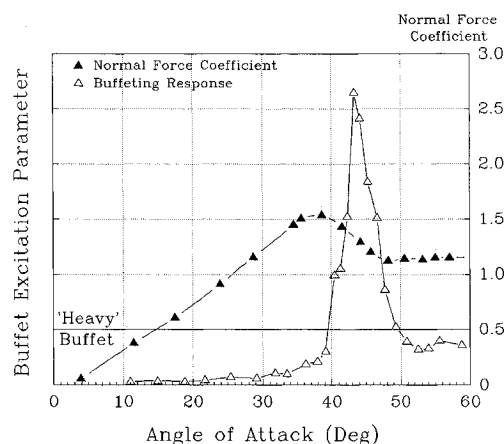


Fig. 5 Buffet profile for unblown wing, first bending mode.

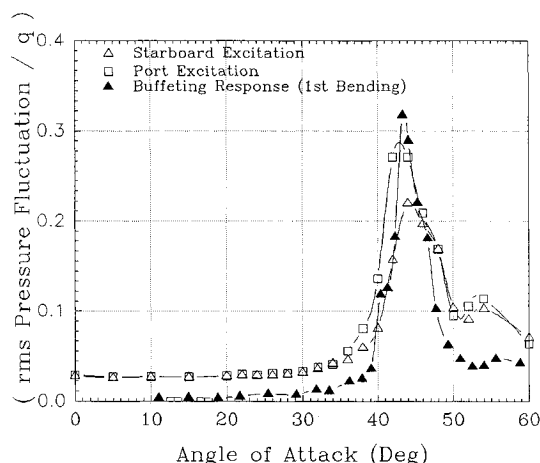


Fig. 6 Comparison between unsteady pressures and buffeting response for unblown wing, first bending mode.

feting increases from this baseline value, up to a sharp peak at  $\alpha = 43$  deg. The severity of the buffet relative to the "heavy" buffet level may suggest that the classification of buffet for wings and fins should be different. The response then falls with increasing angle of attack to reach a fairly constant level, the fin being in the wake of the fully stalled wing (like that of a bluff body). When compared to normal force data for the same wing, it is evident that the point of maximum buffeting occurs in the poststall region. No significant buffeting was recorded in either the first torsional mode or the second bending mode at this tunnel speed.

The rms pressure levels corresponding to the above response are shown in Fig. 6. For  $\alpha < 34$  deg, both port and starboard faces of the fin experience low levels of unsteadiness. The port trace then rises the quicker (perhaps due to some slight sideslip on the fin, or some tunnel swirl) to peak at  $\alpha = 43$  deg, whereas the starboard trace peaks at  $\alpha = 44$  deg. When compared to the buffeting response, it can be seen that the profiles of both sets of curves are very similar.

Typical unsteady pressure fluctuations for both faces of the rigid fin at  $\alpha = 44$  deg are shown in Fig. 7. It can be seen that the traces move in and out of phase regularly. When out of phase, one face of the fin experiences an instantaneous suction, and the other face experiences an instantaneous pressure (and vice versa). For a flexible fin, this would induce a side force and possibly a fin deflection.

This suggests that there is an energy transfer from the flow (in the form of pressure fluctuations) into the structure (in the form of fin deflection). A possible mechanism for this energy transfer can be deduced from the spectra of the unsteady pressures. Figure 8a shows the power spectral density (PSD) function corresponding to the point  $\alpha = 10$  deg in

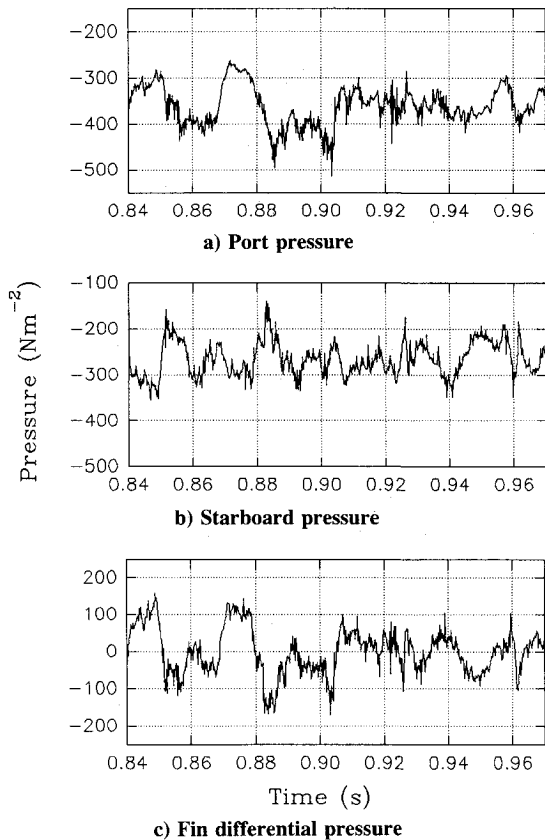


Fig. 7 Unsteady pressure traces,  $\alpha = 44$  deg.

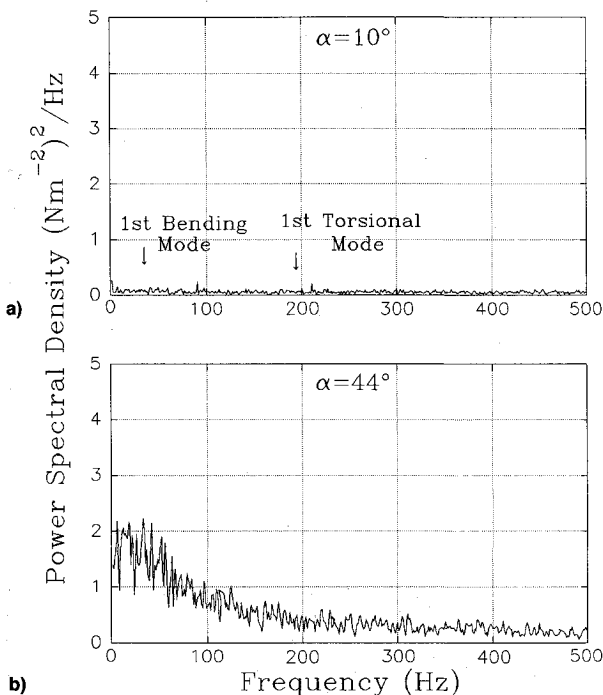


Fig. 8 Power spectral density, unblown wing: a)  $\alpha = 10$  deg and b)  $\alpha = 44$  deg.

Fig. 6 (for the starboard face). It can be seen that the spectrum has no distinct frequencies, and the overall excitation level is much less than Fig. 8b, which corresponds to the point  $\alpha = 44$  deg. The spectrum at peak buffeting reveals a broadband excitation which decreases in intensity to the background level at around  $f = 200$  Hz. The absence of any torsional buffeting is due to the torsional natural frequency (192 Hz) not lying within this excitation range. Conversely, the bending response

was large, since the natural mode was situated inside the excitation band.

The nature of the fin excitation pressures can be analyzed by subtracting the pressure time trace corresponding to one face of the fin from the other. This subtraction emphasizes the out-of-phase components of the pressure traces (and hence, the differential pressure across the fin), and suppresses the effect of any in-phase components (Fig. 7c).

Figure 9 shows the PSD function of the differential pressure trace (port minus starboard) corresponding to the point  $\alpha = 44$  deg (Fig. 7c). It can be seen that a peak occurs at approximately 35 Hz. Therefore, for this model configuration, the spectra of individual pressure transducer outputs on each face of the fin show little distinct periodicity, yet the spectrum of the differential pressure does. This variation of peak vortex excitation frequency is also linear with freestream velocity<sup>8</sup> (as expected).

Figure 10 presents the variation of vortex excitation frequency with freestream velocity for several angles of attack. The curves are linear for all cases. Using a reduced frequency parameter incorporating the vortex excitation frequency ( $f_{\text{VORTEX}}$ ) and a nominal wake width ( $\bar{c} \sin \alpha$ ), it can be seen that the peak vortex excitation frequency can be expressed in the form  $(f_{\text{VORTEX}} \bar{c} / U_\infty) \sin \alpha = \text{const}$  (for a given configuration) (Table 1).

This parameter represents the frequency content of the vortical flow for this wing. Therefore, this model configuration is suggested to exhibit a characteristic value of 0.55 in accordance with a recent study using wings of similar planform.<sup>20</sup> Frequency parameter tests using the flexible fin<sup>21</sup> also give a value of approximately 0.55 (Fig. 11). This shows the

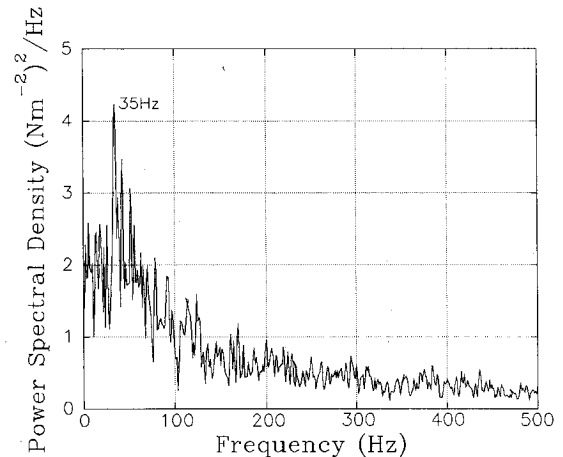


Fig. 9 Power spectral density of fin differential pressure, unblown wing,  $\alpha = 44$  deg.

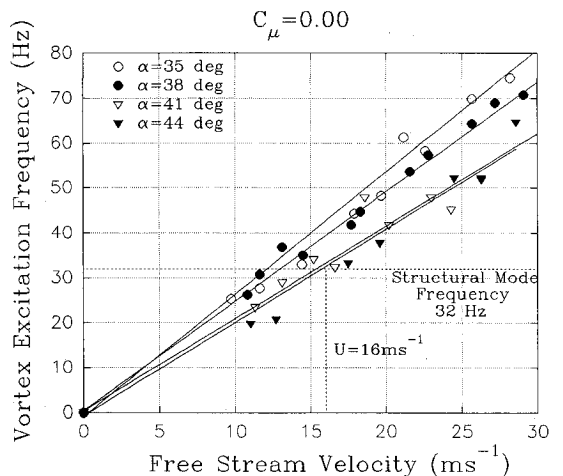
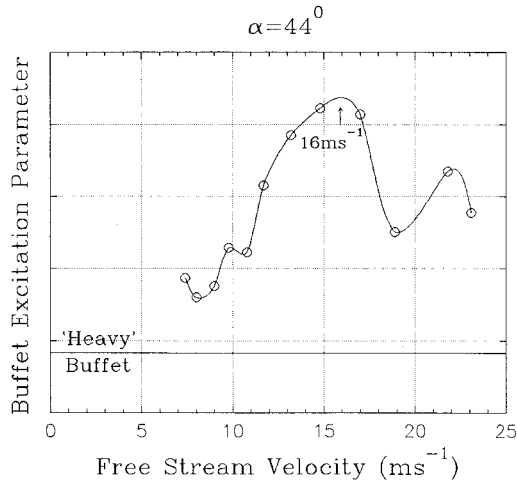


Fig. 10 Variation of vortex excitation frequency with freestream velocity, unblown wing.

**Table 1** Vortex frequency parameters without TLEB

$\alpha$	$(f_{\text{VOTEX}}\bar{c})/U_\infty$	$(f_{\text{VOTEX}}\bar{c})\sin \alpha/U_\infty$
35 deg	0.96	0.55
38 deg	0.89	0.55
41 deg	0.75	0.49
44 deg	0.76	0.53

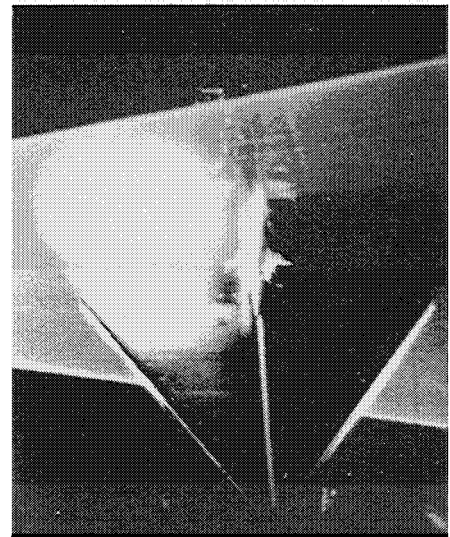
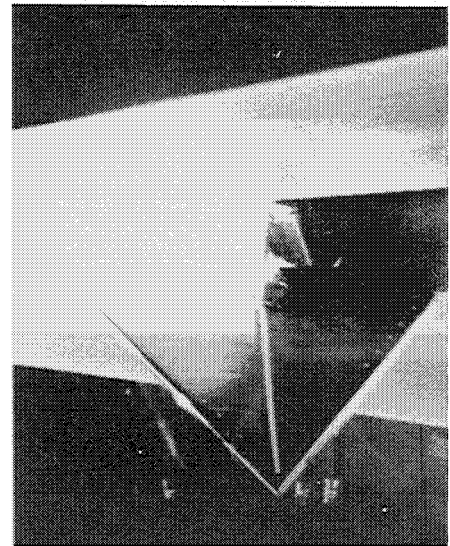
**Fig. 11** Variation of buffeting response with freestream velocity, unblown wing.

variation of buffeting in the fundamental bending mode with freestream velocity. It can be seen that there is a peak in the response at approximately  $16 \text{ ms}^{-1}$ . When transferred onto Fig. 10, it is evident that the dominant vortical flow frequency at  $\alpha = 44$  deg is almost identical to the frequency of the natural mode excited. This confirms that the maximum buffeting response (for a given angle of attack) occurs when the frequency of the excitation flowfield matches the structural mode frequency, as would be expected. However, comparisons between different buffeting studies suggest that  $\bar{c} \sin \alpha$  is not an appropriate scaling parameter, since different values of the reduced frequency parameter are found (0.22,<sup>3</sup> 0.29<sup>8,22</sup> using unsteady pressures, and 0.71<sup>23</sup> using the response).

Laser light sheet flow visualization was performed to establish the flow conditions at various buffeting levels. Figure 12a shows the starboard vortex located away from the fin at  $\alpha = 36$  deg (before peak buffeting). The port vortex is in the shade of the fin, and is therefore not illuminated. At  $\alpha = 43$  deg (Fig. 12b) it can be seen that the leading-edge vortex core diameter has grown, and the vortex-free shear layer is located on or near the fin tip.<sup>24</sup>

Since the laser light sheet image represents a two-dimensional slice through the flow, it is necessary to consider the flow conditions three-dimensionally. As well as impinging on the fin tip, each vortex free shear layer impinges on the swept leading edge of the fin. Video recordings suggest that a vortex/fin interaction is present at maximum buffeting. When the port vortex contracts slightly, the starboard vortex expands (and vice versa) to maintain vortex equilibrium. This may relate to the 180-deg phase lag in the pressure fluctuations discussed earlier. Consequently, the shear layers oscillate across the fin leading edge and tip, resulting in large fin excitations.

Normal force data was acquired for the unblown wing, with and without the fin fitted. It was found that the fin had little effect on the force curves, with lift curve slopes and stall angles remaining constant. Also steady-state static pressure data was taken at angles of attack before and after buffet onset. For all cases, the flow was symmetrical (i.e., no vortex asymmetry), even at maximum buffeting.<sup>24</sup> These observations strongly suggest that the presence of the fin has very little effect on the vortical flow over a delta wing at incidence, as the fin is situated away from the track of either vortex.

**a)  $\alpha = 36$  deg****b)  $\alpha = 43$  deg****Fig. 12** Laser light sheet flow visualization, unblown wing.

### With TLEB

#### Parallel Slot Distribution

The parallel leading-edge slot configuration had a constant slot height of 0.5 mm. Figure 13 shows the single-fin response in the fundamental bending mode for four different values of  $C_\mu$ . For low angles of attack, the effect of blowing is small, since the vortices are located away from the fin. At around  $\alpha = 35$  deg, buffet onset occurs for all cases. The effect of TLEB is to reduce the rate of buffet increase after buffet onset, resulting in the buffeting peak being shifted to a higher angle of attack. As the amount of blowing increases the peaks are offset further from the baseline case with little change in the peak buffeting level. This supports the hypothesis that TLEB reduces the "effective angle of attack" of the vortices. A shift of around 8 deg in the angle at peak buffeting was experienced using a  $C_\mu$  of 0.10.

The effect of  $C_\mu$  on wing normal force is presented in Fig. 14. It can be seen that the blowing increases the potential angle-of-attack range of the wing by approximately 8 deg for  $C_\mu = 0.10$ . Although the maximum value of normal force has reduced with  $C_\mu$ , the TLEB was also seen to reduce the unsteady normal force component.

Laser light sheet flow visualization (Fig. 15) was performed to establish the flow conditions for each peak buffeting case.

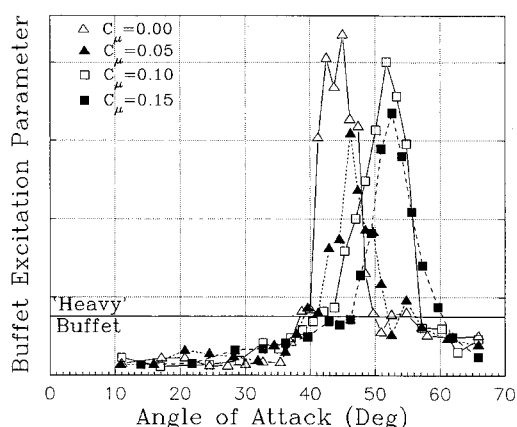


Fig. 13 Effect of blowing momentum coefficient on buffet profiles for blown wing, first bending mode, parallel slot distribution.

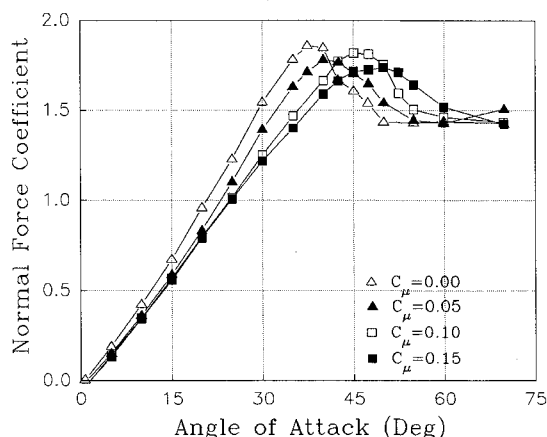


Fig. 14 Effect of blowing momentum coefficient on normal force, blown wing.

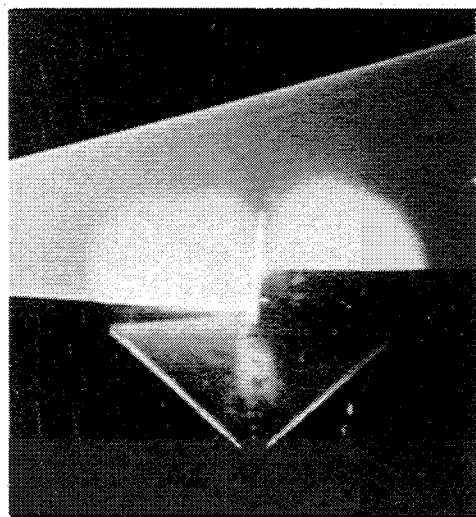


Fig. 15 Laser light sheet flow visualization, blown wing,  $\alpha = 47$  deg,  $C_\mu = 0.05$ .

Figure 15 shows that at  $\alpha = 47$  deg,  $C_\mu = 0.05$  the flow conditions are similar to those in Fig. 12b, emphasizing that the buffeting mechanism has been shifted to a higher angle of attack.

#### Tapering Slot Distribution

The slot height for the tapered configuration varied linearly from 0.05 mm near the wing apex to 0.45 mm near the wing trailing edge. The response profiles for this slot distribution are shown in Fig. 16. In comparison with Fig. 13, it can be seen that both sets of curves exhibit the same trends. How-

ever, the angle-of-attack shift for a particular  $C_\mu$  is much greater when using the tapering slots, as the conicality of the flow has been maintained. For example, for  $C_\mu = 0.10$ , the angle-of-attack shift is around 8 deg for the parallel slot distribution and around 14 deg for the tapering slot. The parallel slot distribution is less efficient as the slot height (and hence, the jet momentum) is too large in comparison to the local wing span at the wing apex and too small towards the wing trailing edge. Therefore, the linear tapering slot distribution is more efficient at modifying the leading-edge vortex characteristics.

The solid line in Fig. 16 represents the buffeting level corresponding to an optimum blowing profile. At  $\alpha = 38$  deg the blowing is steadily increased to  $C_\mu \approx 0.10$  at  $\alpha = 41$  deg (peak buffeting), resulting in lower buffeting levels. As the angle of attack increases further, the blowing is reduced gradually, until at approximately  $\alpha = 48$  deg,  $C_\mu = 0.00$  and the buffeting returns to the unblown level. It is clear that the buffeting peak can be completely suppressed using such a blowing profile.

The effect of TLEB on the spectrum of the differential pressure between the transducers at  $\alpha = 44$  deg is presented in Fig. 17. In comparison with the unblown spectrum (Fig. 9), the blown spectrum still comprises large pressure fluctuations at frequencies less than 200 Hz, but at reduced levels. Consequently, there is a reduction in the buffeting response. When the buffet excitation and response are compared, it is evident that both have been shifted to higher angles of attack, confirming that TLEB has modified only the vortex characteristics.

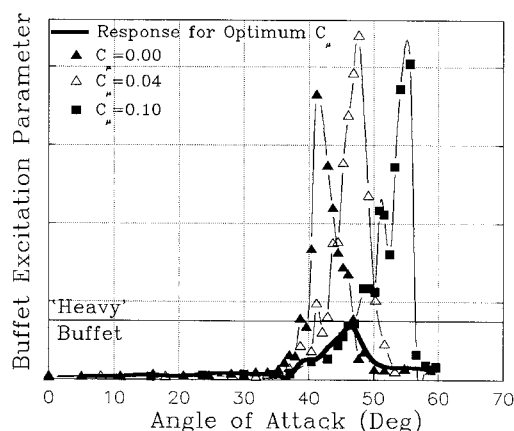


Fig. 16 Effect of blowing momentum coefficient on buffet profiles for blown wing, first bending mode, tapering slot distribution.

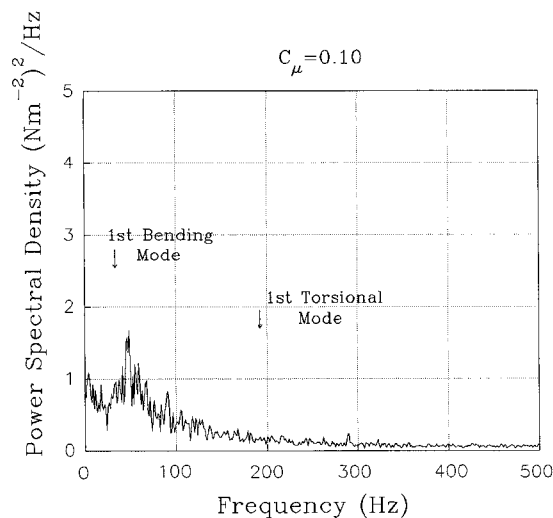


Fig. 17 Power spectral densities for  $\alpha = 44$  deg,  $C_\mu = 0.10$ .

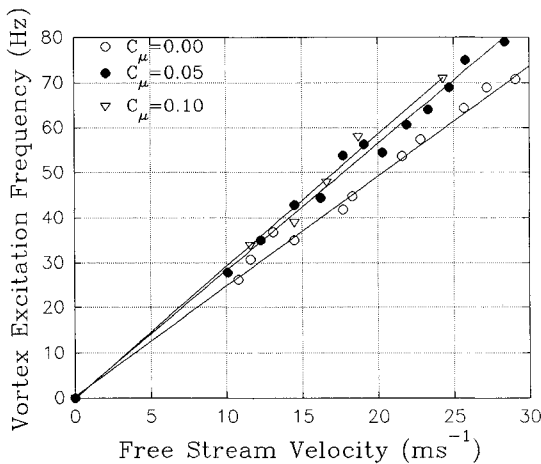


Fig. 18 Effect of symmetric TLEB on vortex excitation frequencies,  $\alpha = 38$  deg.

Table 2 Vortex frequency parameters with symmetric TLEB

$\alpha$	$(f_{\text{VORTEX}}\bar{c})/U_\infty$	$(f_{\text{VORTEX}}\bar{c})\sin \alpha/U_\infty$
$C_\mu = 0.05$		
38 deg	1.03	0.63
42 deg	0.95	0.63
46 deg	0.85	0.61
50 deg	0.72	0.55
$C_\mu = 0.10$		
38 deg	1.09	0.67
42 deg	0.98	0.66
46 deg	0.96	0.69
50 deg	0.90	0.69

Figure 18 shows the effect of symmetric TLEB on the vortex excitation frequency for  $\alpha = 38$  deg. All curves are linear, and the gradients of the lines increase with increasing  $C_\mu$ . The results corresponding to tests conducted at several angles of attack are presented in Table 2.

Hence, symmetric TLEB has shifted the vortex reduced frequency parameter to larger values to 0.62 ( $C_\mu = 0.05$ ) and 0.68 ( $C_\mu = 0.10$ ). Scaled upon the sine of the angle of attack, these new characteristic values correspond to reductions in the effective angle of attack of 7 and 14 deg, respectively. These reductions compare favorably with the positive angle-of-attack shifts in the buffeting response, which were induced by the blowing. The shift of reduced frequency parameter is therefore equivalent to a reduction of the vortical flow angle of attack for a wing of given sweep. This analogy is much simplified, and more work needs to be done to verify the effect of TLEB on leading-edge vortices.

Mass flow requirements for TLEB are comparable to short-takeoff vertical landing reaction control systems; for a modern combat aircraft at low speeds typical of a high angle-of-attack flight, a total  $C_\mu$  of 0.10 corresponds to about 10% of compressor mass flow. Possible increases in blowing efficiency with reduced slot height may reduce mass flow requirements. Depending on engine rating philosophy, this level of bleed may not necessarily give proportional thrust losses.

### Conclusions

A system to suppress single-fin buffeting on a simple delta wing has been designed, built, and tested, with suppression achieved at any angle of attack. It has been shown that the frequency content of the excitation flowfield is a function of freestream velocity and angle of attack. When using a characteristic length ( $\bar{c} \sin \alpha$ ), the value of this function (for unblown single-finned configurations) is approximately 0.55.

Symmetric TLEB induces a linear shift in the buffeting response and the wing stall angle. It was found that a tapering slot was almost twice as efficient at modifying vortex behavior, and therefore, suppressing fin buffeting, compared to a parallel slot.

The maximum response was characterized by both leading-edge vortex shear layers impinging on the fin leading edge and tip.

### References

- Herbst, W. B., "Future Fighter Technologies," *Journal of Aircraft*, Vol. 17, No. 8, 1980, pp. 561–566.
- Orlik-Rückemann, K. J., "Aerodynamic Aspects of Aircraft Dynamics at High Angles of Attack," *Journal of Aircraft*, Vol. 20, No. 9, 1983, pp. 737–752.
- Triplett, W. E., "Pressure Measurements on Twin Vertical Tails in Buffeting Flow," AIAA Paper 82-0641, Jan. 1982.
- Wentz, W. H., Jr., "Vortex-Fin Interaction on a Fighter Aircraft," AIAA Paper 87-2474, Aug. 1987.
- Ross, A. J., Jefferies, E. B., and Edwards, G. F., "Aerodynamic Data for the Effects of Nose Suction on a High Incidence Research Model with a Large Forebody," Royal Aircraft Establishment TM 2204, UK, Jan. 1991.
- Lee, B. H. K., and Brown, D., "Wind Tunnel Studies of F/A-18 Tail Buffet," AIAA Paper 90-1432, June 1990.
- Lee, B. H. K., and Brown, D., "Wind Tunnel Investigation and Flight Tests of Tail Buffet on the CF-18 Aircraft," AGARD CP-483, Paper 1, Sorrento, Italy, April 1990.
- Martin, C. A., Glaister, M. K., MacLaren, L. D., Meyn, L. A., and Ross, S., "F/A-18 1/9th Scale Model Tail Buffet Measurements," Aeronautical Research Lab. Flight Mechanics Rept. 188, June 1991.
- Mabey, D. G., and Pyne, C. R., "Reduction of Fin Buffeting by Tangential Blowing on the Leading Edge of a Wing," Defence Research Agency TM 2215, May 1991.
- Greenwell, D. I., and Wood, N. J., "Control of Asymmetric Vortical Flows," AIAA Paper 91-3272, Sept. 1991.
- Shi, Z., Wu, J. M., and Vakili, A. D., "An Investigation of Leading-Edge Vortices on Delta Wings with Jet Blowing," AIAA Paper 87-0330, Jan. 1987.
- Anglin, E. L., and Satran, D., "Effects of Spanwise on Two Fighter Airplane Configurations," *Journal of Aircraft*, Vol. 17, No. 12, 1980, pp. 883–889.
- Visser, K. D., Iwanski, K. P., Nelson, R. C., and Ng, T. T., "Control of Leading Edge Vortex Breakdown by Blowing," AIAA Paper 88-0504, Jan. 1988.
- Trebbles, W. J. G., "Exploratory Investigation of the Effects of Blowing from the Leading Edge of a Delta Wing," NASA Ames Research Center R&M 3518, April 1966.
- Wood, N. J., and Roberts, L., "The Control of Delta Wing Aerodynamics at High Angles of Attack," *The Prediction and Exploitation of Separated Flows*, Royal Aeronautical Society, April 1989.
- Wood, N. J., "Development of Lateral Control on Aircraft Operating at High Angles of Attack," International Council of the Aeronautical Sciences 90-5.6.3, Sept. 1990.
- Greenwell, D. I., Bean, D. E., and Wood, N. J., "A High Angle of Attack Model Support System for the 7' x 5' Wind Tunnel," Mechanical Engineering Rept. 50/1992, Univ. of Bath, Bath, England, UK, July 1992.
- Wood, N. J., Roberts, L., and Lee, K. T., "The Control of Vortical Flow on a Delta Wing at High Angles of Attack," AIAA Paper 87-2278, Aug. 1987.
- Mabey, D. G., "Some Aspects of Aircraft Dynamic Loads Due to Flow Separation," AGARD R-750, May 1988.
- Chapman, M., and Cheeseman, J., "Vortex Burst Frequencies," School of Mechanical Engineering Rept. AE10/92, Univ. of Bath, Bath, England, UK, April 1992.
- Wood, N. J., "Suppression of Vortex Induced Unsteady Loads at High Angles of Attack," School of Mechanical Engineering Progress Rept., Univ. of Bath, Bath, England, UK, Oct. 1991.
- Zimmerman, N. H., Ferman, M. A., Yurkovich, R. N., and Gestenkorn, G., "Prediction of Tail Buffet Loads for Design Application," AIAA Paper 89-1378, April 1989.
- Mabey, D. G., and Pyne, C. R., "Buffeting on the Single Fin of a Combat Aircraft Configuration at High Angles of Incidence," Royal Aircraft Establishment TR 91006, UK, Jan. 1991.
- Bean, D. E., and Wood, N. J., "An Experimental Investigation of Empennage Buffeting," AIAA Paper 91-3224, Sept. 1991.